

pubs.acs.org/joc Article

Computational Exploration of the Thermal Rearrangement of Basketene: One Forbidden versus Two Allowed Pericyclic Reactions

Xiaolin Yue, Qingyang Zhou, and K. N. Houk*



Cite This: J. Org. Chem. 2023, 88, 14303-14307



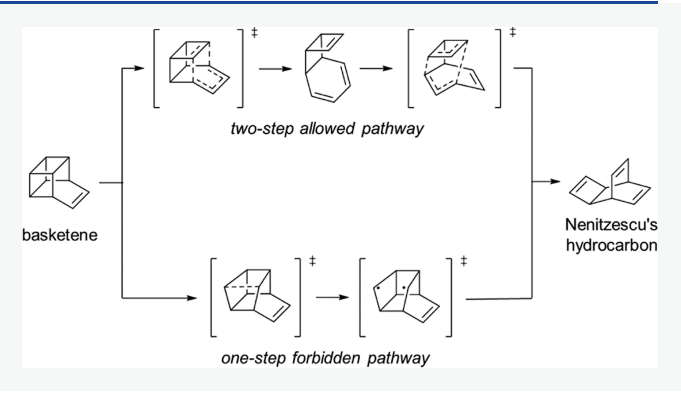
ACCESS

III Metrics & More

Article Recommendations

Supporting Information

ABSTRACT: The thermal rearrangement of basketene to Nenitzescu's hydrocarbon has been explored using density functional theory (M06-2X and ω B97X-D) and DLPNO–CCSD-(T) quantum mechanics. Both the sequential thermally allowed retro Diels–Alder followed by Cope rearrangement and the thermally forbidden retro-[2 + 2] cycloaddition were studied. The controlling role of orbital symmetry rather than reaction thermodynamics is demonstrated.



■ INTRODUCTION

Basketene, or pentacyclo $[4.4.0.0^{2.5}.0^{3.8}.0^{4.7}]$ dec-9-ene, is a polycyclic $C_{10}H_{10}$. The name derives from its structural similarity to that of a basket. Basketene was first synthesized in 1966 both by Masamune and Dauben. The synthetic route starts from the Diels—Alder cycloaddition of cyclooctatetraene to maleic anhydride, followed by a photochemical [2 + 2] cycloaddition to close the cage structure and finally saponification and decarboxylation (Figure 1). The successful synthesis of basketene laid the foundation for further experimental studies on its transformations, especially pericyclic reactions.

Figure 1. Synthesis of basketene.

As a member of the $(CH)_n$ hydrocarbon family, basketene can be converted to many isomers that share the $(CH)_{10}$ formula. Famously, basketene (1) undergoes thermal rearrangements to form Nenitzescu's hydrocarbon (3). The reaction can also be catalyzed by the rhodium catalyst $(I)^2$ or $LiCB_{11}Me_{12}$. The mechanism is known to involve two allowed pericyclic reactions: a retro Diels–Alder reaction,

followed by a [3,3] sigmatropic shift, also known as Cope rearrangement (Figure 2A).^{4,5} The measured activation parameters for the first step are $\Delta H^{\ddagger}=29$ kcal/mol, $\Delta S^{\ddagger}=1$ e.u.⁴ and those for the second step are $E_a=23.5\pm1$ kcal/mol, log $A=11.5.^{5}$ Converted to free energies, ΔG^{\ddagger} barriers are 28.6 kcal/mol (110 °C, in CD₃CN) and 25.5 kcal/mol (55 °C) for the two steps, respectively. The first step is the rate-determining step.

The mechanism involves this two-step allowed pathway instead of a one-step forbidden yet direct pathway (Figure 2B).⁴ The first proof is the lack of evidence for a diradical species. Emission and absorption from chemically induced dynamic polarization were not observed in the olefinic protons of 3, a phenomenon otherwise expected in processes involving diradicals. Second, isotopic labeling experiments align with the two-step pathway. The proposed mechanism leads to the deuterium distribution shown in 3', the thermal rearrangement product of deuterium-labeled compound 1' (Figure 2C). Finally, the kinetic study and trapping are consistent with the multistep mechanism. The reaction of compound 1 with tetracyanoethylene (TCNE) led to adduct 4, and the rate constant was, within experimental error, equal to that of the thermolysis in the absence of TCNE. Therefore, step a should

Received: May 4, 2023
Published: September 28, 2023





Figure 2. (A) Mechanism for the thermal rearrangement reaction of basketene through the retro Diels—Alder reaction, followed by a Cope rearrangement. (B) Alternative mechanism of a forbidden yet direct retro-[2 + 2] reaction. (C) Experiments and the TCNE trapping result supporting the allowed two-step mechanism.⁴

be the rate-determining step in the overall rearrangement pathway.

As computer hardware and algorithms advance and play an increasingly indispensable role, density functional theory (DFT) and wavefunction methods have been widely applied to provide probative evidence for mechanism studies and, specially, to determine between stepwise and concerted pathways. Although various experimental and computational studies have been performed on (CH)₁₀ hydrocarbons recently, none involved a study of the rearrangement mechanism. We now report a computational study of the thermal rearrangement of basketene to Nenitzescu's hydrocarbon using DFT (M06-2X and ω B97X-D) and DLPNOCCSD(T) to determine the favored mechanism and how strain and orbital symmetry factors influence the mechanism.

Computational Methods. Geometry optimizations and frequency calculations were performed with the M06-2X density functional¹⁰ and def2-SVP basis set,¹¹ while the def2-TZVPP basis set¹¹ was used for single point energies. All calculations were performed using the Gaussian 16 program.¹² Transition states were distinguished as having only one imaginary frequency and were verified by intrinsic reaction coordinate (IRC) calculations.¹³ ωB97X-D¹⁴ was also applied as a comparison to the M06-2X functional. Single point energy calculations were also performed at the DLPNO–CCSD-(T)¹⁵/def2-TZVPP level of theory using ORCA¹⁶ to obtain accurate results. Free energies were all corrected to 1 mol/L, and Grimme's quasi-harmonic approach was used.¹⁷ Frequency correction were performed using the GoodVibes program.¹⁸ 3D renderings of structures were illustrated using CYLview.¹⁹

RESULTS AND DISCUSSION

The mechanism involving two concerted pericyclic reactions is shown in Figure 3A. Free energy barriers were calculated using

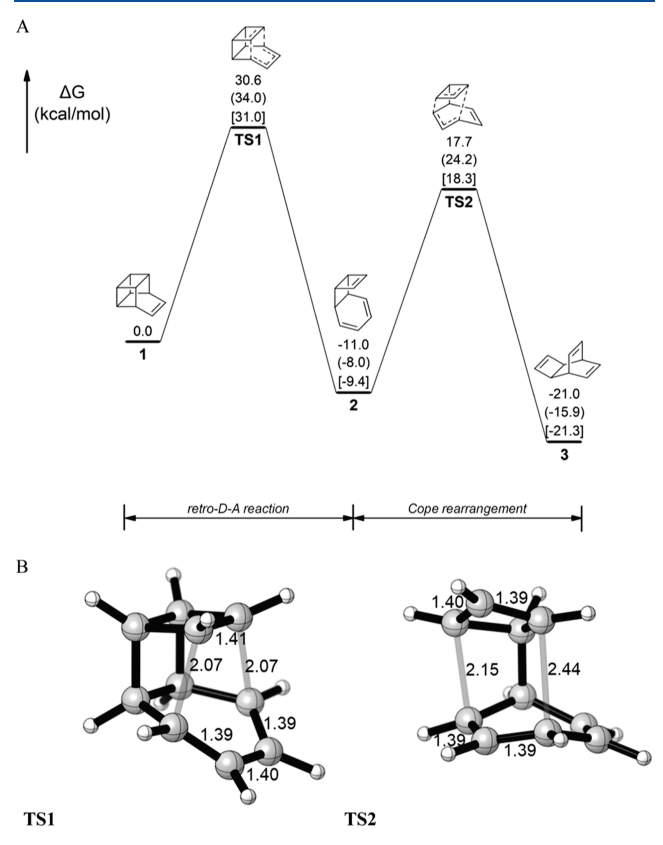


Figure 3. (A) Free energy barriers of the two-step pericyclic pathway calculated by three different quantum mechanics methods, M06-2X, ω B97X-D in round brackets, and DLPNO–CCSD(T) in square brackets. (B) Structures of transition states **TS1** and **TS2** in the allowed pericyclic pathway. The structures are optimized by M06-2X/def2SVP. Bond lengths are in Å.

three representative quantum mechanics methods. 20 M06-2X and DLPNO–CCSD(T) generated barriers of $\sim\!31$ and 28–29 kcal/mol versus 29 and 26 kcal/mol experimentally, respectively. ω B97X-D values are 34 and 32, respectively, about 5 kcal/mol too high. Therefore, the M06-2X functional was selected as the best method, given full consideration to both the accuracy and computation cost.

The free energy barriers of the two allowed steps are 30.6 and 28.7 kcal/mol, respectively, showing the first step as the rate-determining step, which is consistent with the kinetics study. The two steps are exergonic by 11.0 and 10.0 kcal/mol, respectively. Geometries of the transition states are shown in Figure 3B. In both of these allowed pericyclic transition states, the bond lengths of partially formed double bonds are 1.39 to 1.41 Å, respectively, about the same as the C–C bond length in benzene (1.39 Å). The bond lengths of partial single bonds fluctuate in a small range from 2.1 to 2.4 Å, which fall in the general region between a single bond (~1.5 Å) and a broken bond (~3.5 Å).

To understand the role of the ring strain in the allowed pathway, the retro Diels—Alder reaction of cyclohexene was studied computationally (Figure 4A) as an unstrained model to compare with the retro Diels—Alder reaction of basketene (Figure 4B). Cyclohexene is first converted from the stable

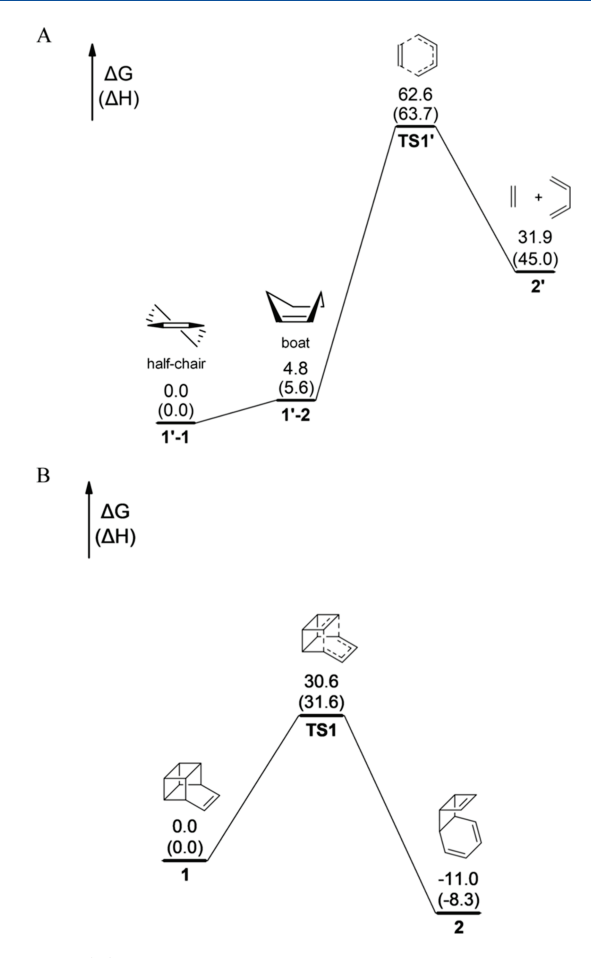


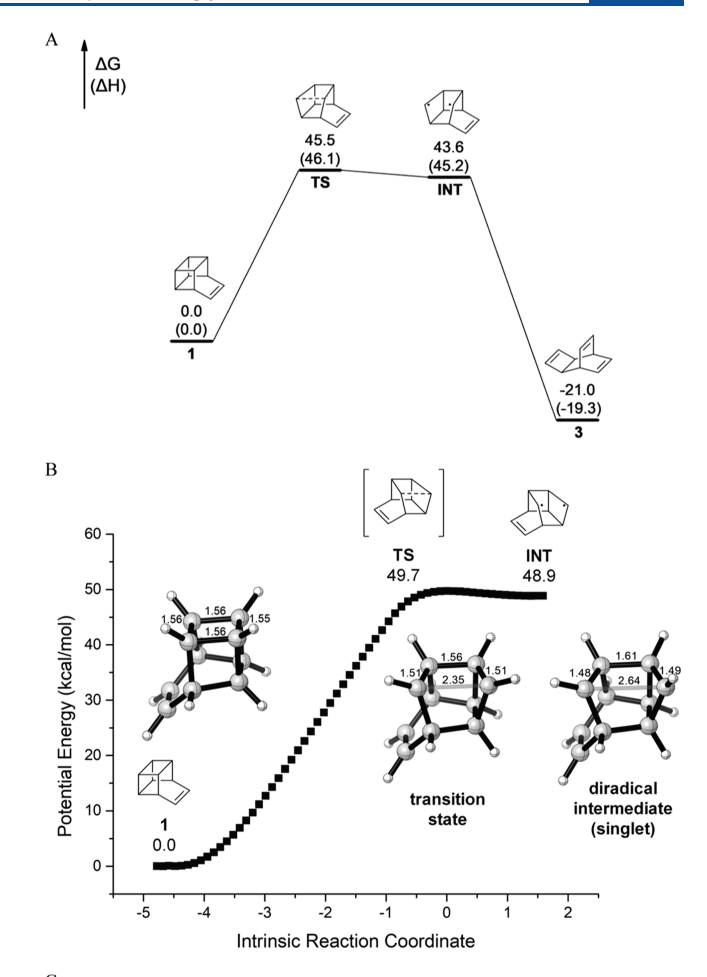
Figure 4. (A) Energetics of the parent retro Diels—Alder reaction starting from cyclohexene. (B) Energetics of the retro Diels—Alder reaction of basketene. The energies are calculated by M06-2X/def2-TZVPP//M06-2X/def2SVP and are in kcal/mol.

half-chair form 1'-1 into the boat form 1'-2, which is the same conformation as the cyclohexene ring in basketene. Comparing ΔH values, the ring opening via the retro Diels—Alder reaction has a barrier of 58.1 kcal/mol versus 31.6 kcal/mol for basketene. The latter is 26.5 kcal/mol lower, which is related to the 47.7 kcal/mol greater exothermicity of the latter reaction, due to strain relief.

To assess the importance of Woodward–Hoffmann rules in establishing the mechanism, the forbidden but direct pathway by a retro $[\pi^2 s + \pi^2 s]$ cycloaddition (Figure 5A) is compared to the observed two-step process. A clear example of the importance of orbital symmetry control, and its transcendence over thermodynamics, is that 1 undergoes a reaction to 2 that is exergonic by only 11.0 kcal/mol by an orbital symmetry allowed retro Diels–Alder cycloaddition, while the alternative formation of 3 by a retro-[2+2] cycloaddition is exergonic by 21.0 kcal/mol, but its barrier is 14.9 kcal/mol higher due to forbidden orbital symmetry.

The cleavage of the first bond has a free energy barrier of 45.5 kcal/mol. Figure 5B shows that TS connects the reactant and a very shallow diradical intermediate. The breaking C–C bond length is 2.35 Å at the TS.

The reaction from INT to 3 is a relatively facile process with a significant reaction barrier. The IRC indicates a high energy barrier for the formation of 3 and a shallow minimum after TS, which is similar to the potential energy surface (PES) in



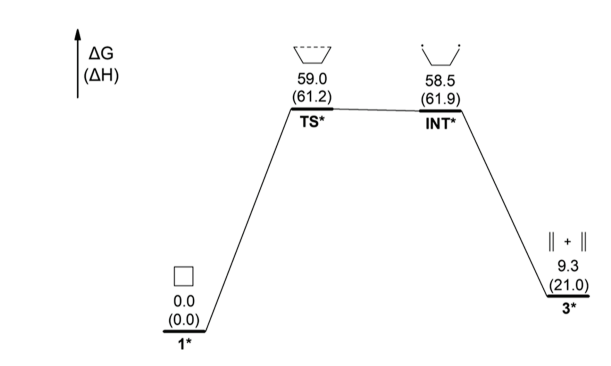


Figure 5. (A) Energetics of the diradical direct pathway. (B) IRC study of the forbidden pathway and the structure of the transition state **TS** and diradical intermediate **INT**. (C) Energetics of the retro-[2 + 2] reaction of cyclobutane.

Doubleday's study of the retro-[2 + 2] cycloaddition of cyclobutane to form two ethylenes. Figure 5C summarizes this. Starting from the intermediate *gauche minimum* tetramethylene diradical, cyclobutane is formed via a single or double conrotatory CH₂ twist, the latter having a tiny barrier of 0.5 kcal/mol shown in Figure 5C. As for basketene, confined by the polycyclic structure, the process from INT to basketene (1) has a calculated barrier of 1.9 kcal/mol, which is comparable to the Doubleday result.

Singlet diradicals are essentially unstable since there is intrinsically no significant barrier for forming a single bond from two radical centers. In DFT calculations, however, there may be false barriers due to massive stabilization or steric

hindrance that prevent radical interactions. Here, the 0.8 kcal/mol barrier in the PES likely results from the need to planarize the radical and induce a strong overlap with the other radical center in TS.

While the ring opening of cyclobutane to two ethylenes is endergonic by 9.3 kcal/mol, the reaction of basketene releases 21.0 kcal/mol of energy. In addition, the free energy barrier for the ring opening of basketene is 13.5 kcal/mol lower than the 59.0 kcal/mol barrier of cyclobutane, a result of strain acceleration. However, this barrier is still not low enough to compete with the allowed reaction, which has a strain relief of 38.1 kcal/mol and a strain acceleration of 27.2 kcal/mol, as noted earlier.

The potential influences of the solvent and substituent effects were also examined briefly. The polarities of the reactant and transition state are very low since this is a pure hydrocarbon and undergoes a nonionic rearrangement mechanism. As a result, the solvent effect is insignificant, as shown in Table 1. Substituent effects were computed for cyano

Table 1. Free Energy Barriers with Frequency Corrections for Cope Rearrangement (TS2) in Different Solvents (Given in kcal/mol) Computed at the $\omega B97X\text{-}D/\text{def2-TZVPP}//\omega B97X\text{-}D/\text{def2-SVP}$ Level of Theory at 298.15 K and 1 mol/L a

solvent	free energy barrier from 2 to TS2
no solvent (gas phase)	32.2
acetonitrile	32.5
ethyl acetate	32.5
tetrahydrofuran	32.5
benzene	32.6
cyclohexane	32.6

^aThe results show that the polarity of solvents has little influence on the energy barrier, even smaller than the accuracy of the computing methods.

and amino groups as representative electron-withdrawing and electron-donating groups. The results are given in Table 2. For the first step, the retro Diels—Alder reaction, the result aligns with the expectation for substituent effects in Diels—Alder reactions. When the dienophile is substituted by CN (1-3-CN and 1-6-CN, which are mirror images) or the diene is substituted with NH₂ (1-10-NH₂), the free energy barrier is

Table 2. Using Substituted Basketene (Noted as 1-n-R, Where n is the Number of the Substituted Atoms and R is the Substituent Group) as the Starting Material, Free Energy Barriers for the First Step (TS1) and the Second Step (TS2) in the Two-step Allowed Pathway (Given in kcal/mol) are Computed at the M06-2X/def2-TZVPP//M06-2X/def2-SVP Levels of Theory

	free energy barriers	
starting material	1 to TS1	2 to TS2
1	30.6	28.7
1-3-CN	29.7	28.6
$1-3-NH_2$	31.3	28.6
1-6-CN	29.7	28.5
1-6-NH ₂	31.3	30.5
1-10-CN	30.8	26.9
1-10-NH ₂	25.9	28.4

lowered by about 1 and 5 kcal/mol, respectively. When the dienophile is substituted by an amino group (1-3-NH₂ and 1-6-NH₂) or the diene is substituted with a cyano group (1-10-CN), the barrier is slightly increased by 1 kcal/mol or negligibly (Table 2). For the second step, the [3,3] sigmatropic shift, CN groups at C6 and C10 lower the barrier by 0.2 and 1.8 kcal/mol, respectively, while amino increases the barrier by 1.8 at C6 and decreases it by 0.3 kcal/mol at C10. At C3, CN and NH₂ reduce the barrier by very little, 0.1 kcal/mol. These substituent effects are in part caused by stabilizing effects on the double bonds in ground states or influences on the rather dissociative style transition states for the Cope rearrangement shown in Figure 3-TS2.

CONCLUSIONS

We calculated the allowed and forbidden mechanisms for the thermal rearrangement reaction of basketene to Nenitzescu's hydrocarbon. A two-step symmetry allowed pathway is found to be much better than a forbidden yet direct process, as expected but now defined quantitatively. This reiterates the predominance of orbital symmetry over thermodynamics in the establishment of mechanisms; here, two 10 kcal/mol exergonic reactions occur by the allowed pathway much more readily than one 20 kcal/mol exergonic forbidden process. The free energy barrier of multistep retro Diels-Alder, Cope mechanism is 14.9 kcal/mol lower than that of the one-step forbidden retro-[2 + 2] reaction. We also revealed that the ring strain in basketene accelerates the retro Diels-Alder reaction by 27.2 kcal/mol and facilitates the retro-[2 + 2] reaction by 13.5 kcal/mol. In conclusion, the concerted pericyclic pathway is the most favorable mechanism, due primarily to an orbital symmetry controlled electronic preference, in spite of the greater strain relief in the retro-[2 + 2] pathway.

ASSOCIATED CONTENT

Data Availability Statement

The data underlying this study are available in the published article and its Supporting Information.

Supporting Information

The Supporting Information is available free of charge at https://pubs.acs.org/doi/10.1021/acs.joc.3c00993.

Calculation details of DLPNO-CCSD(T); Cartesian coordinates and electronic energies of optimized structures; comparison of free energy barriers with different functionals; and calculation on solvent effects and substituent effects (PDF)

AUTHOR INFORMATION

Corresponding Author

K. N. Houk — Department of Chemistry and Biochemistry, University of California, Los Angeles, California 90095, United States; orcid.org/0000-0002-8387-5261; Email: houk@chem.ucla.edu

Authors

Xiaolin Yue — School of Chemical Engineering and Technology, Tianjin University, Tianjin 300350, China; College of Chemistry,, Nankai University, Tianjin 300071, China

Qingyang Zhou – Department of Chemistry and Biochemistry, University of California, Los Angeles, California 90095, United States Complete contact information is available at: https://pubs.acs.org/10.1021/acs.joc.3c00993

Notes

The authors declare no competing financial interest.

ACKNOWLEDGMENTS

We are grateful to the National Science Foundation (CHE-2153972 to K.N.H.) for financial support of this research. Calculations were performed on the IDRE (Institute of Digital Research and Education) Hoffman2 Cluster at the University of California, Los Angeles.

REFERENCES

- (1) (a) Masamune, S.; Cuts, H.; Hogben, M. G. Strained systems. VII. Pentacyclo[4.2.2.0^{2,5}.0^{3,8}.0^{4,7}]deca-9-ene, basketene. *Tetrahedron Lett.* **1966**, 7, 1017–1021. (b) Dauben, W. G.; Whalen, D. L. Pentacyclo[4.4.0.02,5.03,8.04,7]decane and pentacyclo-[4.3.0.0^{2,5}.0^{3,8}.0^{4,7}]nonane. *Tetrahedron Lett.* **1966**, 7, 3743–3750.
- (2) Dauben, W. G.; Schallhorn, C. H.; Whalen, D. L. Synthesis and rearrangement of strained cage molecules. *J. Am. Chem. Soc.* **1971**, 93, 1446–1452.
- (3) Moss, S.; King, B. T.; de Meijere, A.; Kozhushkov, S. I.; Eaton, P. E.; Michl, J. LiCB₁₁Me₁₂: A Catalyst for Pericyclic Rearrangements. *Org. Lett.* **2001**, *3*, 2375–2377.
- (4) Westberg, H. H.; Cain, E. N.; Masamune, S. Thermolysis of pentacyclo [4.4.0.0.2,50.3,804,7] dec-9-ene. *J. Am. Chem. Soc.* **1969**, *91*, 7512–7514.
- (5) Vedejs, E. Tricyclo[4,1,0.0^{2,5}]deca-3,7,9-triene. *J. Chem. Soc. D* 1971, 536–537.
- (6) Tran, Q.; Sengupta, A.; Houk, K. N. Probative Evidence and Quantitative Energetics for the Unimolecular Mechanism of the 1,5-Sigmatropic Hydrogen Shift of Cyclopentadiene. *J. Org. Chem.* **2022**, 87, 14995–15000.
- (7) Svatunek, D.; Pemberton, R. P.; Mackey, J. L.; Liu, P.; Houk, K. N. Concerted [4 + 2] and Stepwise (2 + 2) Cycloadditions of Tetrafluoroethylene with Butadiene: DFT and DLPNO-UCCSD(T) Explorations. J. Org. Chem. 2020, 85, 3858–3864.
- (8) Verevkin, S. P.; Kümmerlin, M.; Hickl, E.; Beckhaus, H.-D.; Rüchardt, C.; Kozhushkov, S. I.; Haag, R.; Boese, R.; Benet-Bucholz, J.; Nordhoff, K.; de Meijere, A. Thermochemical and X-ray Crystallographic Investigations of Some (CH)₁₀ Hydrocarbons: Basketene, Nenitzescu's Hydrocarbon, and Snoutene. *Eur. J. Org Chem.* **2002**, 2002, 2280–2287.
- (9) Touš, P.; Červinka, C. Dynamic Disorder, Strain, and Sublimation of Crystalline Caged Hydrocarbons from First Principles. *Cryst. Growth Des.* **2023**, 23, 4082–4097.
- (10) Zhao, Y.; Truhlar, D. G. The M06 suite of density functionals for main group thermochemistry, thermochemical kinetics, noncovalent interactions, excited states, and transition elements: two new functionals and systematic testing of four M06-class functionals and 12 other functionals. *Theor. Chem. Acc.* 2008, 120, 215–241.
- (11) Weigend, F.; Ahlrichs, R. Balanced Basis Sets of Split Valence, Triple Zeta Valence and Quadruple Zeta Valence Quality for H to Rn: Design and Assessment of Accuracy. *Phys. Chem. Chem. Phys.* **2005**, *7*, 3297–3305.
- (12) Frisch, M. J.; Trucks, G. W.; Schlegel, H. B.; Scuseria, G. E.; Robb, M. A.; Cheeseman, J. R.; Scalmani, G.; Barone, V.; Petersson, G. A.; Nakatsuji, H.; Li, X.; Caricato, M.; Marenich, A. V.; Bloino, J.; Janesko, B. G.; Gomperts, R.; Mennucci, B.; Hratchian, H. P.; Ortiz, J. V.; Izmaylov, A. F.; Sonnenberg, J. L.; Williams-Young, D.; Ding, F.; Lipparini, F.; Egidi, F.; Goings, J.; Peng, B.; Petrone, A.; Henderson, T.; Ranasinghe, D.; Zakrzewski, V. G.; Gao, J.; Rega, N.; Zheng, G.; Liang, W.; Hada, M.; Ehara, M.; Toyota, K.; Fukuda, R.; Hasegawa, J.; Ishida, M.; Nakajima, T.; Honda, Y.; Kitao, O.; Nakai, H.; Vreven, T.; Throssell, K.; Montgomery, J. A.; Peralta, J. E.; Ogliaro, F.; Bearpark, M. J.; Heyd, J. J.; Brothers, E. N.; Kudin, K. N.; Staroverov, V. N.;

- Keith, T. A.; Kobayashi, R.; Normand, J.; Raghavachari, K.; Rendell, A. P.; Burant, J. C.; Iyengar, S. S.; Tomasi, J.; Cossi, M.; Millam, J. M.; Klene, M.; Adamo, C.; Cammi, R.; Ochterski, J. W.; Martin, R. L.; Morokuma, K.; Farkas, O.; Foresman, J. B.; Fox, D. J. *Gaussian 16*; revision A.03; Gaussian Inc: Wallingford, CT, 2016.
- (13) Fukui, K. The Path of Chemical Reactions—the IRC Approach. *Acc. Chem. Res.* **1981**, *14*, 363–368.
- (14) Chai, J. D.; Head-Gordon, M. Long-Range Corrected Hybrid Density Functionals with Damped Atom-Atom Dispersion Corrections. *Phys. Chem. Chem. Phys.* **2008**, *10*, 6615–6620.
- (15) Raghavachari, K.; Trucks, G. W.; Pople, J. A.; Head-Gordon, M. A fifth-order perturbation comparison of electron correlation theories. *Chem. Phys. Lett.* **1989**, *157* (6), 479–483.
- (16) (a) Neese, F. The ORCA program system. Wiley Interdiscip. Rev.: Comput. Mol. Sci. 2012, 2 (1), 73–78. (b) Neese, F. Software update: the ORCA program system, version 4.0. Wiley Interdiscip. Rev.: Comput. Mol. Sci. 2017, 8 (1), No. e1327.
- (17) Grimme, S. Supramolecular Binding Thermodynamics by Dispersion-Corrected Density Functional Theory. *Chem.—Eur. J.* **2012**, *18*, 9955–9964.
- (18) Luchini, G.; Alegre-Requena, J. V.; Funes-Ardoiz, I.; Paton, R. S. GoodVibes: Automated Thermochemistry for Heterogeneous Computational Chemistry Data. F1000Research 2020, 9, 291.
- (19) Legault, C. Y. CYLview20; Université de Sherbrooke, 2020. http://www.cylview.orwebg.
- (20) Mardirossian, N.; Head-Gordon, M. Thirty years of density functional theory in computational chemistry: an overview and extensive assessment of 200 density functionals. *Mol. Phys.* **2017**, *115*, 2315–2372.
- (21) Sexton, T.; Kraka, E.; Cremer, D. Extraordinary Mechanism of the Diels—Alder Reaction: Investigation of Stereochemistry, Charge Transfer, Charge Polarization, and Biradicaloid Formation. *J. Phys. Chem. A* **2016**, *120*, 1097–1111.
- (22) Doubleday, C., Jr. Tetramethylene. J. Am. Chem. Soc. 1993, 115, 11968–11983.